Journal of Alloys and Compounds 509 (2011) 9986–9991

Contents lists available at ScienceDirect

Journal of Alloys and Compounds

journal homepage: www.elsevier.com/locate/jallcom

Low-temperature sintering and dielectric properties of high-permittivity microwave (Ca, Nd)TiO_3 ceramics

Qi-long Zhang, Hui-ping Sun, Hui Yang*

Department of Materials Science and Engineering, Zhejiang University, Hangzhou 310027, China

ARTICLE INFO

Article history:
Received 4 February 2011
Received in revised form 3 August 2011
Accepted 3 August 2011
Available online 10 August 2011

Keywords:
Ceramics
Sintering
Electronic properties
X-ray diffraction

ABSTRACT

The effect of H_3BO_3–CuO–Li_2CO_3 combined additives on the sintering temperature, microstructure and microwave dielectric properties of $(Ca_{0.61}Nd_{0.26})(Ti_{0.98}Sn_{0.02})O_3$ (CNTS) ceramics was investigated. The H_3BO_3–CuO–Li_2CO_3 combined additives lowered the sintering temperature of CNTS ceramics effectively from 1300 to 950 °C. This may be due to the interim liquid-phase of Li_2O–CuO–B_2O_3, which were formed in the sintering process. $(Li_{0.5}Nd_{0.5})TiO_3$ (LNT) demonstrated an effective compensation in τ_f value of the low-fired CNTS ceramics. The 0.4CNTS–0.6LNT ceramics with 5 wt% (H_3BO_3–CuO)–0.5 wt% Li_2CO_3 sintered at 900 °C for 2 h shows excellent dielectric properties: $\varepsilon_r = 90.6$, $Q \times f = 3400$ GHz, and $\tau_f = 9$ ppm/°C. Also, the LTCC material is compatible with Ag electrode.

1. Introduction

Recently, considerable attention has been paid to the development of the low-temperature co-fired ceramics (LTCC) for the benefits offered to the fabrication of miniature multilayer devices. In order to process ceramics with electrode material, such as silver (melting point = 961 °C), it is required to sinter the dielectrics at temperatures lower than the melting temperature of the co-fired electrode material. Several LTCC microwave dielectric ceramics such as (Zn, Ba)O–Nb_2O_5, NO–SiO_2 (N = Mg, Zn, Ca), RO–V_2O_5 (R = Sr, Ba, Mg), BaO–Nb_2O_5–TiO_2, $SrCuSi_4O_{10}$, $LiAlSiO_4$, $Li_2MgTi_3O_8$, $Ca[(Li_{1/3}Nb_{2/3})_{1-x}Ti_x]O_{3-\delta}$, etc., have been reported [1–25]. However, most of the reported LTCC microwave dielectric ceramics show medium or low dielectric constant (<70). Comparatively, LTCC microwave dielectric ceramics with high-permittivity, which are used in miniature multilayer components such as filters, antennas and baluns, have not been extensively studied.

High-permittivity microwave dielectric ceramics mainly include BaO–R_2O_3–TiO_2 (R = Nd, Sm), (Pb, Ca)(Fe, Nb)O_3, $(Ca_{1-x}Nd_{2x/3})TiO_3$, CaO–Li_2O–Ln_2O_3–TiO_2, SrO–CeO_2–TiO_2, etc. [26–35]. Among these materials, $(Ca_{1-x}Nd_{2x/3})TiO_3$, a solid solution of CaO, Nd_2O_3 and TiO_2, has been viewed as a potential candidate material because of its high dielectric constant. At microwave frequency range, for $x = 0.39$, it exhibits a good quality factor $Q \times f$ value ~17,200 GHz, a high dielectric constant $\varepsilon_r \sim 108$, and a temperature coefficient of resonant frequency $\tau_f \sim 270$ ppm/°C [36]. With doping $Li_{1/2}Nd_{1/2}TiO_3$ which has larger negative τ_f, $0.55(Ca_{0.61}Nd_{0.26})TiO_3$-$0.45Li_{1/2}Nd_{1/2}TiO_3$ ceramics is found to yield $\varepsilon_r \sim 101$, $Q \times f \sim 5300$ GHz, and a low $\tau_f \sim 13$ ppm/°C due to the temperature compensating effect of mixed compositions [37]. However, the sintering temperature of $(Ca_{1-x}Nd_{2x/3})TiO_3$ is above 1400 °C, which is too high to be applicable to LTCC. So it is necessary to reduce the sintering temperature. Wei et al. lowered the sintering temperature of $(Ca_{1-x}Nd_{2/3x})TiO_3$ ceramics to 880 °C by adding $3ZnO{\cdot}2B_2O_3$ glass [38]. Unfortunately, the ε_r and Q values were drastically decreased ($\varepsilon_r = 30$–60, $Q = 200$–550) due to the glass with low ε_r and high dissipation factor, besides, the ceramics showed large τ_f of 20–60 ppm/°C.

In this work, for improving the dielectric properties of lower-temperature sintering $(Ca_{0.61}Nd_{0.26})(Ti_{0.98}Sn_{0.02})O_3$ (CNTS) ceramics, the multiple additive consisting of H_3BO_3–CuO–Li_2CO_3 (BCL)were added to CNTS ceramics to decrease the sintering temperature, and negative τ_f value ceramics $(Li_{0.5}Nd_{0.5})TiO_3$ (LNT) as compensators were introduced. The dense low-firing microwave ceramics with superior dielectric properties was obtained. The chemical compatibility between the LTCC materials and electrodes has also been investigated.

2. Experimental procedures

Calcium carbonate ($CaCO_3$, 99%), titanium oxide (TiO_2, 99.9%), neodymium oxide (Nd_2O_3, 99.9%), tin oxide (SnO_2, 99.5%), boric acid (H_3BO_3, 99.5%), copper oxide (CuO, 99%), and lithium carbonate (Li_2CO_3, 98%) were used as starting materials. The starting materials were weighed according to the compositions $(Ca_{0.61}Nd_{0.26})(Ti_{0.98}Sn_{0.02})O_3$ (CNTS) and $(Li_{0.5}Nd_{0.5})TiO_3$ (LNT), and milled with zirconia balls for 24 h in ethanol and then dried. The CNTS and LNTS powders were calcined at 1100 °C

* Corresponding author. Tel.: +86 571 87951408; fax: +86 571 87953054.
E-mail address: mse237@zju.edu.cn (H. Yang).

0925-8388/$ – see front matter © 2011 Elsevier B.V. All rights reserved.
doi:10.1016/j.jallcom.2011.08.005

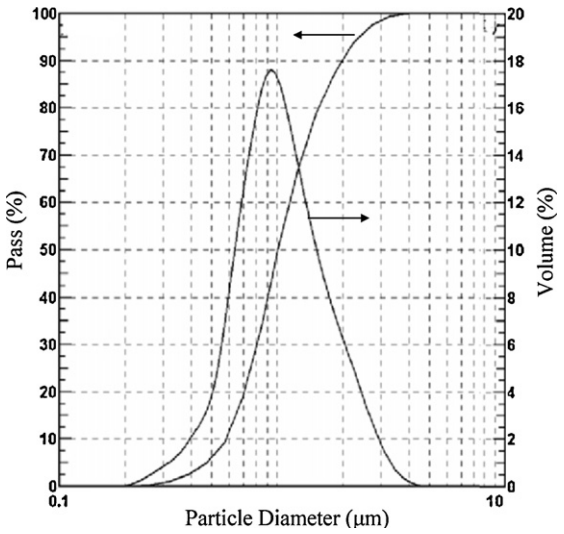

Fig. 1. The particle size distribution of the milled powders.

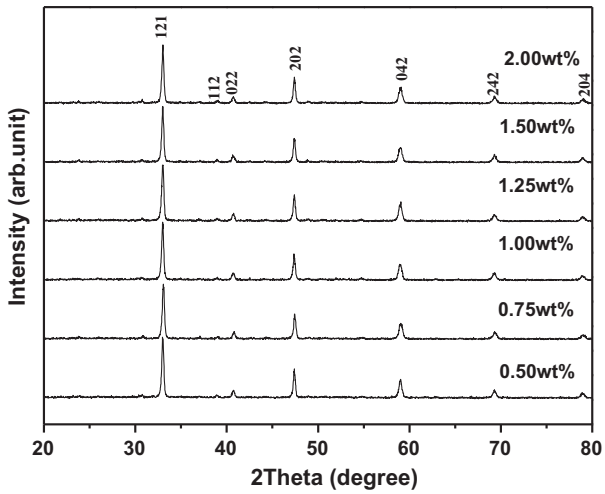

Fig. 2. XRD patterns of CNTS ceramics with 5 wt% (H_3BO_3–CuO)–x wt% Li_2CO_3 sintered at 950 °C for 2 h.

for 4 h in a sealed crucible. The calcined reagents were re-milled for 16 h according to the formulas of CNTS with 5 wt% (H_3BO_3–CuO)–x wt% Li_2CO_3 ($0.5 \le x \le 2.0$) and $(1-y)$ CNTS-y LNT ($0.4 \le y \le 0.7$) with 5 wt% (H_3BO_3–CuO)–0.5 wt% Li_2CO_3, respectively. Fig. 1 shows the particle size distribution of the milled powders. The distribution of particles volume average diameter D_{50} is 1.01 μm. After drying and sieving, the admixtures were uniaxially pressed under a pressure of 100 MPa into disks of 18 mm in diameter and 9 mm in thickness. The pellets covered with crucible were sintered in air at 875–975 °C for 2 h.

Powder X-ray diffraction (XRD) data were collected on a RIGAKU D/max 2550 PC (Rigaku Co., Tokyo, Japan) with Cu Kα radiation. XRD data were acquired over a range of $2\theta = 10°$–$80°$ with a step size of 0.02° and a count time of 2 s. The bulk densities and porosities of the sintered samples were measured by the Archimedes method. For microstructural examination, the sintered ceramics were polished and thermally etched (100 °C below the sintering temperature) in air for 30 min. The microstructure analyses of the sintered surface were performed using a scanning electron microscopy (SEM, FEI SIRION-100, Netherlands) and an energy dispersive X-ray spectroscopy (EDS, Horiba EMAX Energy, EX-350). Dielectric constant (ε_r) and quality factor values at microwave frequency ($Q \times f$) were measured using Hakki–Coleman method and cavity method by vector network analysis (Agilent 8719ET, USA), respectively. The temperature coefficient of resonant frequency (τ_f) can be calculated by noting the variation of resonant frequency of the TE_{011} resonant mode over the temperature of 25–80 °C.

3. Results and discussion

Fig. 2 shows the XRD patterns of CNTS ceramics with 5 wt% (H_3BO_3–CuO)–x wt% Li_2CO_3 addition sintered at 950 °C for 2 h. $CaCO_3$, Nd_2O_3 and TiO_2 formed $GdFeO_3$-type orthorhombic perovskite phase, which was agreed with that reported by Yoshida et al. [34]. Sn substitution in the B site ions could form complete solid solutions. There are no evidence of any secondary phases like CuO, B_2O_3, $Li_2B_4O_7$ and $LiBO_2$. It is possible that H_3BO_3–CuO–Li_2CO_3 (BCL) liquid phase was not crystallized during cooling and remained as the amorphous phase, or the secondary phase was too small to be detected by routine powder XRD.

Fig. 3 illustrates the relative densities of the CNTS ceramics with 5 wt% (H_3BO_3–CuO)–x wt% Li_2CO_3 as a function of sintering temperature from 900 to 975 °C for 2 h. The relative densities of the CNTS ceramics increase initially with increasing the sintering temperature and then almost saturate at above 950 °C. The relative densities of CNTS ceramics with BCL sintered at 950 °C were almost the same as the undoped CNTS ceramic sintered at 1350 °C (95.6% of calculated theoretical density). Obviously, after adding the BCL, the sintering temperature of the CNTS ceramics has been efficiently decreased by approximately 400 °C. The highest relative density could be obtained for the CNTS ceramics with 5 wt% (H_3BO_3–CuO)–0.5 wt% Li_2CO_3 sintered at 975 °C. However, further increasing Li_2CO_3 content led to a slight decrease in the relative density. The SEM micrographs of the CNTS ceramics with 5 wt% (H_3BO_3–CuO)–x wt% Li_2CO_3 addition sintered at 950 °C for 2 h are illustrated in Fig. 4. All the specimens showed dense microstructures with little porosity. It can be seen that a large number of quadrate grains (1–2 μm) and a few sheet grains (3–4 μm in length) coexisted in BCL-doped CNTS ceramics. With increasing the x content, the number of sheet grains was decreased, but there were no significant differences in the number and size of pores.

Table 1 shows the dielectric properties of CNTS ceramics with 5 wt% (H_3BO_3–CuO)–x wt% Li_2CO_3 addition sintered at 950 °C for 2 h. With increasing the x content, the ε_r values increased and the $Q \times f$ values decreased. As we know, the microwave dielectric loss includes not only intrinsic losses which were mainly contributed by the lattice vibrational modes but also extrinsic losses caused by densification/porosity, secondary phases, grain sizes and oxygen vacancies. Moreover, the $Q \times f$ value was independent of density or porosity for a relative density higher than 90% [39]. Since the relative densities of CNTS ceramics with BCL sintered at 950 °C were higher than 94%, the $Q \times f$ values decreased with increasing the amount of Li_2CO_3 addition, which is attributed to the increase of liquid phase with high dielectric loss and Li volatilization [40]. As shown in Table 1, the higher the content of Li_2CO_3 addition is, the lower the τ_f of the CNTS samples resulted. As the Li_2CO_3 content

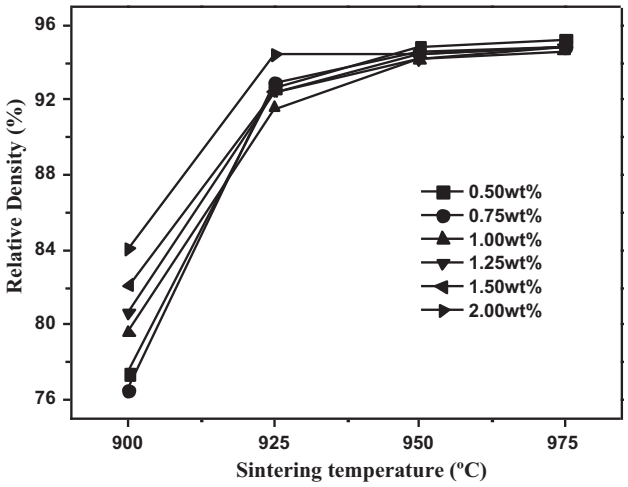

Fig. 3. Relative densities of CNTS ceramics with 5 wt% (H_3BO_3–CuO)–x wt% Li_2CO_3 as a function of sintering temperature from 900 to 975 °C for 2 h.

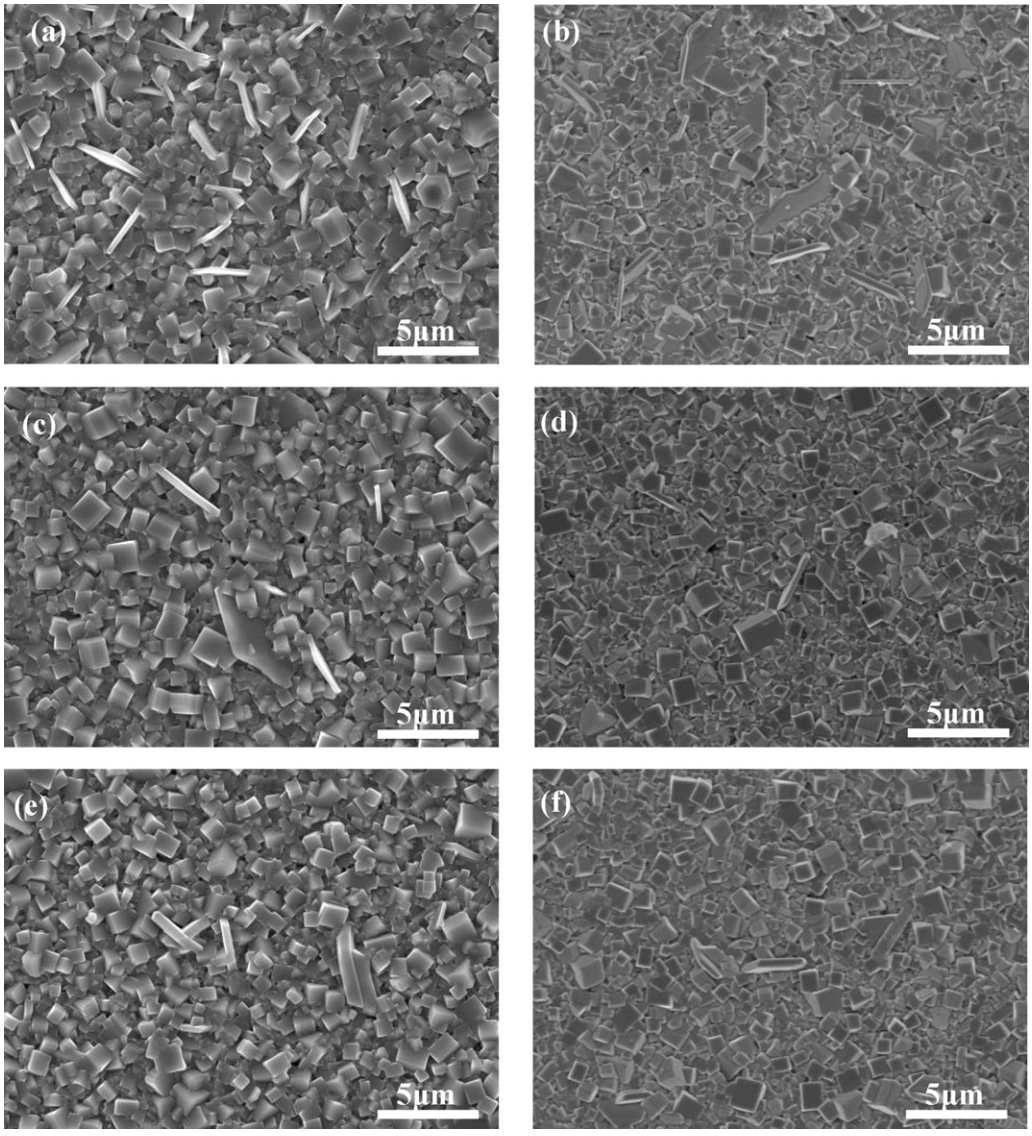

Fig. 4. SEM micrographs of CNTS ceramics with 5 wt% (H_3BO_3–CuO)–x wt% Li_2CO_3 sintered at 950 °C for 2 h: (a) x = 0.50, (b) x = 0.75, (c) x = 1.0, (d) x = 1.25, (e) x = 1.50 and (f) x = 2.0.

increased from 0.5 to 2 wt%, the τ_f value decreased from 183 to 124 ppm/°C. The decrease in τ_f might be due to liquid phases having a lower τ_f.

Fig. 5 shows the DTA–TG curve of 5 wt% (H_3BO_3–CuO)–2 wt% Li_2CO_3 addition. The endothermic peaks around 153 °C and 174 °C, associated with a large weight loss of about 28% between approximately 87 °C and 226 °C in the TG curve, is due to the decomposition of H_3BO_3 into HBO_2 and B_2O_3. A broad exothermic peak at 566 °C is accompanied by another weight loss in the TG curve. The XRD

Table 1
Dielectric properties of CNTS ceramics with 5 wt% (H_3BO_3–CuO)–x wt% Li_2CO_3 sintered at 950 °C for 2 h.

x wt% Li_2CO_3	Microwave dielectric properties		
	ε_r	$Q \times f$ (GHz)	τ_f (ppm/°C)
0.5	94.6	8300	183
0.75	95.5	8010	180
1.0	96.1	7550	172
1.25	97.6	6890	160
1.5	98.9	6570	144
2.0	102.1	5260	124

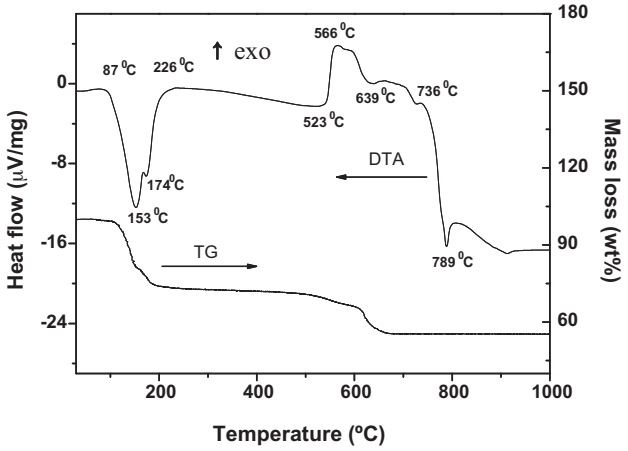

Fig. 5. DTA–TG curve of 5 wt% (H_3BO_3–CuO)–2 wt% Li_2CO_3 additive.

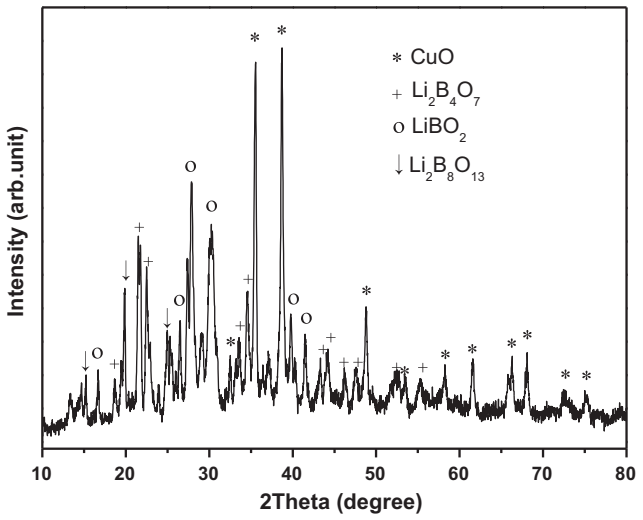

Fig. 6. XRD patterns of the 5 wt% (H_3BO_3–CuO)–2 wt% Li_2CO_3 additive calcined at 600 °C for 2 h.

patterns of 5 wt% (H_3BO_3–CuO)–2 wt% Li_2CO_3 heat-treated at 600 °C for 2 h are shown in Fig. 6. The CuO, $Li_2B_4O_7$, $LiBO_2$ and $Li_2B_8O_{13}$ phases were observed. It indicates that the weight loss at 600 °C is due to the reaction between $LiCO_3$ and B_2O_3 and the release of CO_2. Above 650 °C, there is almost no weigh loss in the TG curve, which suggests that the reaction has finished. The endothermic peak around 789 °C is associated with the transition of admixture from solid-phase to liquid phase. X-ray analysis in Fig. 2 shows that only single perovskite phase was obtained. It could be concluded that $Li_2B_4O_7$, $LiBO_2$ and $Li_2B_8O_{13}$ phases firstly were produced at 600 °C. Then the reaction phases such as $Li_2B_4O_7$, together with CuO, might form the low-melting liquid phase which improves the CNTS ceramics sintering. Moreover, the liquid phase remained as the amorphous phase in the ceramics, which was not detected by XRD.

In order to acquire the closer zero τ_f, LNT was added to CNTS with 5 wt% (H_3BO_3–CuO)–0.5 wt% Li_2CO_3. X-ray diffraction (XRD) patterns of the $(1-y)$ CNTS–yLNT ceramics with 5 wt% (H_3BO_3–CuO)–0.5 wt% Li_2CO_3 sintered at 900 °C for 2 h are shown in Fig. 7. CNTS and LNT ceramics exhibited the structures of

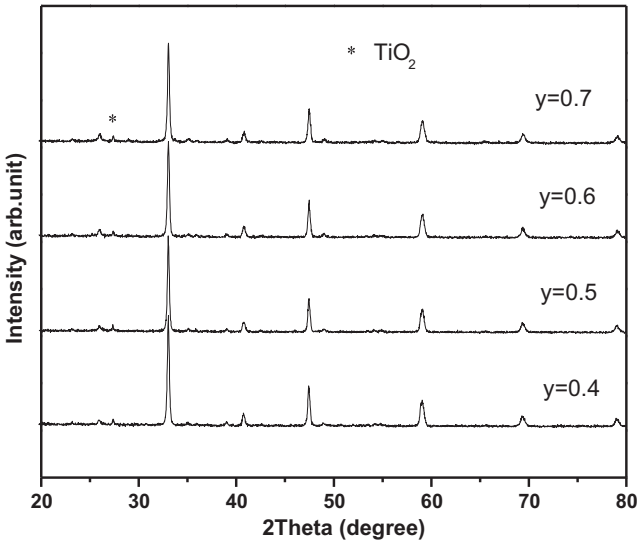

Fig. 7. X-ray diffraction (XRD) patterns of the $(1-y)$CNTS–yLNT ceramics with 5 wt% (H_3BO_3–CuO)–0.5 wt% Li_2CO_3 sintered at 900 °C for 2 h.

Table 2
Relative densities, porosities and dielectric properties of $(1-y)$CNTS–yLNT ceramics with 5 wt% (H_3BO_3–CuO)–0.5 wt% Li_2CO_3 sintered at 900 °C for 2 h.

LNT (y)	Relative density (%)	Porosity (%)	Microwave dielectric properties		
			ε_r	$Q\times f$ (GHz)	τ_f (ppm/°C)
0.4	96.55	0.48	92.8	3880	75
0.5	96.98	0.52	90.9	3660	34
0.6	97.63	0.51	90.6	3400	9
0.7	96.96	0.44	84.2	3250	−41

orthorhombic and cubic, respectively. The perovskite structure was identified with secondary phase TiO_2 for all compositions tested in the experiment. The forming of the second phase TiO_2, which would affect the dielectric properties of CNTS-LNT ceramics, might be due to the Li volatilization. However, the second phase TiO_2 has no significant change at higher LNT content. SEM micrographs of the $(1-y)$CNTS–yLNT ceramics with 5 wt% (H_3BO_3–CuO)–0.5 wt% Li_2CO_3 sintered at 900 °C for 2 h are illustrated in Fig. 8. The grains are closely packed and a small amount of porosity can be observed. A narrow grain size distribution was observed for $y=0.4$, with the grain sizes of quadrate grains in the range of 0.5–1 μm. Two types grain morphology: small quadrate and large rod-like grains, were clearly visible for $y=0.5$–0.7. The number of large rod-like grains increased with increasing the LNT content. In order to identify the phase composition of grains, EDS was used for $y=0.7$. The EDS datum of spots A and B are shown in Fig. 9. The quadrate grains contained Ca, Nd and rich-Ti, while the rod-like grains showed Ti, Nd and Sn. Thus, the quadrate grains and rod-like grains are probably corresponding to perovskite structure (Ca, Nd)TiO_3 and (Li, Nd)TiO_3 phase, respectively, which is confirmed that the rod-like grains increased with the increase of LNT content.

Table 2 shows the relative densities and dielectric properties of $(1-y)$ CNTS–yLNT ceramics with 5 wt% (H_3BO_3–CuO)–0.5 wt% Li_2CO_3 sintered at 900 °C for 2 h. All specimens sintered at 900 °C showed very high relative density (>96% of the theoretical density). The porosities of $(1-y)$ CNTS–yLNT ceramics were lower than 0.61% in all cases and spanned in the range from 0.54 to 0.61%. From the comparison of Table 2 and Fig. 3, it can be seen that, adding to the same BCL, the sintering temperature of $(1-y)$CNTS–yLNT compound ceramics is lower than that of CNTS ceramics due to the lower sintering temperature of LNT (~1250 °C) [41]. As x value increased from 0.4 to 0.7, the τ_f values of ceramics varied from 75 to −41 ppm/°C. Since the τ_f went through zero, it indicates that zero τ_f value can be obtained by adjusting the y value of $(1-y)$CNTS–yLNT ceramics. The ε_r and $Q\times f$ values decreased with increasing y owing to lower permittivity (~80) and quality factor $Q\times f$ (~2500 GHz) of LNT ceramics. Typically, the 0.4CNTS–0.6LNT ceramics with 5 wt% (H_3BO_3–CuO)–5 wt% Li_2CO_3 sintered at 900 °C for 2 h exhibited good dielectric properties of $Q\times f=3400$ GHz, $\varepsilon_r=90.6$, and $\tau_f=9$ ppm/°C. Compared to the dielectric properties of ZnO–B_2O_3 glass-added $(Ca_{1-x}Nd_{2/3x})TiO_3$ ceramics ($\varepsilon_r=30$–60, $Q=200$–550, $\tau_f=20$–60 ppm/°C) [38], BCL-doped CNTS–LNT ceramics have higher ε_r and $Q\times f$ values, but lower τ_f.

To verify whether or not the silver electrode reacts with the dielectric, 5 wt% (H_3BO_3–CuO)–5 wt% Li_2CO_3-added 0.4CNTS–0.6LNT thick film that printed Ag paste (7251D, Namics) was cofired at 900 °C for 2 h, and interactions between the low-firing samples and electrodes were analyzed. Fig. 10 shows the SEM image and energy-dispersive spectrum (EDS) of the interface of ceramic sheet with Ag electrode and the corresponding Ag distribution. It is obvious that the ceramic layer and the electrode layer are compatible and almost no crack exists at the interface between them. Ag is distributed in the central conductor

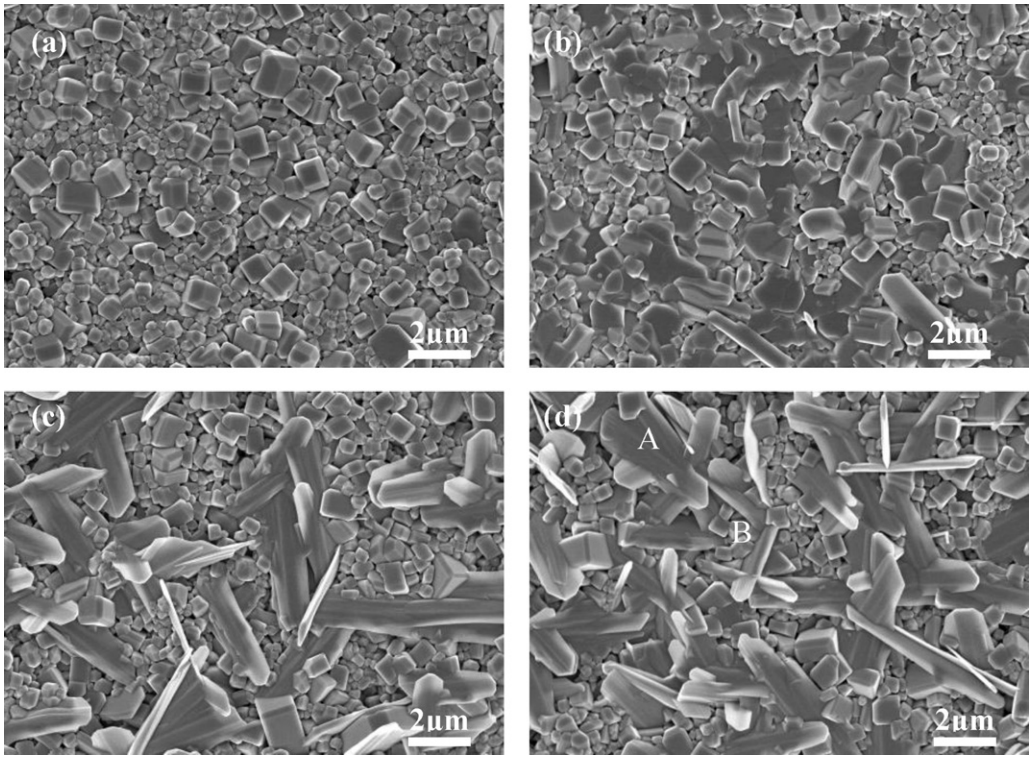

Fig. 8. SEM micrographs of the $(1-y)$CNTS–yLNT ceramics with 5 wt% (H_3BO_3–CuO)–0.5 wt% Li_2CO_3 sintered at 900 °C for 2 h: (a) $y = 0.4$, (b) $y = 0.5$, (c) $y = 0.6$ and (d) $y = 0.7$.

region and does not diffuse into the ceramic region. Overall, it is concluded that the low-fired 0.4CNTS–0.6LNT ceramics is able to match the Ag electrode well. Therefore, the 0.4CNTS–0.6LNT ceramics with 5 wt% (H_3BO_3–CuO)–5 wt% Li_2CO_3 additives could be selected as suitable candidates for LTCC materials, due to low sintering temperature, good microwave dielectric properties, and compatibility with electrodes.

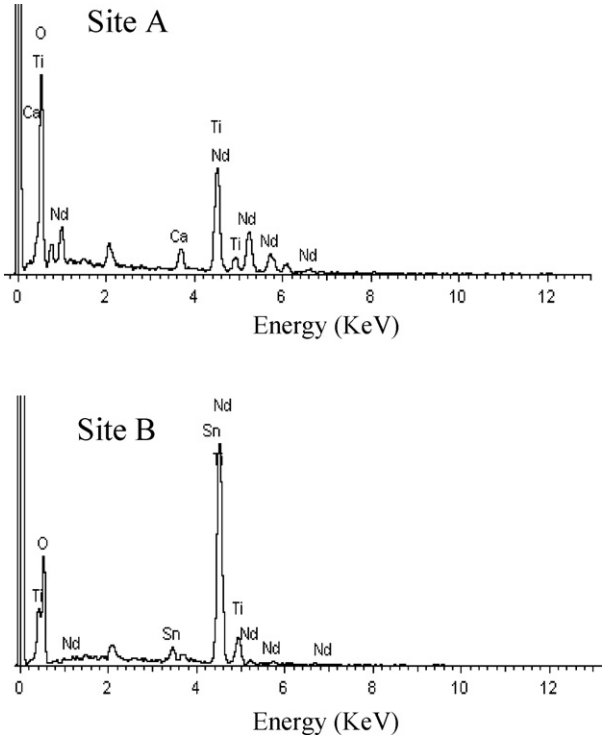

Fig. 9. EDS analysis of 0.3 CNTS–0.7 LNT ceramics with 5 wt% (H_3BO_3–CuO)–0.5 wt% Li_2CO_3 sintered at 900 °C for 2 h.

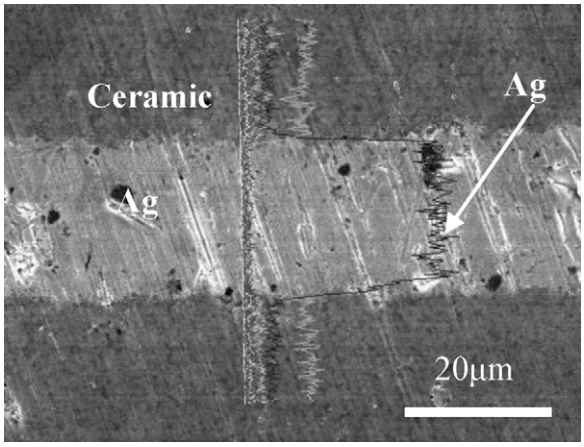

Fig. 10. SEM micrograph and EDS of 0.4CNTS–0.6LNT ceramics with 5 wt% (H_3BO_3–CuO)–5 wt% Li_2CO_3 co-fired with Ag in air at 900 °C for 2 h.

4. Conclusions

In this study, the effect of H_3BO_3–CuO–Li_2CO_3 additives on the sintering temperature, microstructures and microwave dielectric properties of $(Ca_{0.61}Nd_{0.26})(Ti_{0.98}Sn_{0.02})O_3$ (CNTS) ceramics were investigated. The H_3BO_3–CuO–Li_2CO_3 combined additives were effective in lowering the sintering temperature (T_s), and dense CNTS ceramics could be obtained at $T_s \leq 950$ °C due to the interim liquid-phase of Li_2O–CuO–B_2O_3, which were formed in the sintering process. $(Li_{0.5}Nd_{0.5})TiO_3$ (LNT) demonstrated an effective compensation in τ_f value of the low-fired CNTS ceramics. The 0.4CNTS–0.6LNT ceramics with 5 wt% (H_3BO_3–CuO)–0.5 wt% Li_2CO_3 sintered at 900 °C for 2 h shows excellent dielectric

properties: $\varepsilon_r = 90.6$, $Q \times f = 3400$ GHz, and $\tau_f = 9$ ppm/°C. Also, the dielectric ceramics shows a good compatibility with the Ag electrode, which is a promising candidate material for LTCC application.

Acknowledgements

The authors thankfully acknowledge the financial support from National Key Technology Support Program (No. 2009BAG12A07).

References

[1] M.T. Sebastian, H. Jantunen, Int. Mat. Rev. 53 (2008) 5357–5390.
[2] H.F. Zhou, H. Wang, M.H. Zhang, H.B. Yang, J. Mater. Res. 25 (2010) 1793–1798.
[3] L. Fang, D.J. Chu, H.F. Zhou, X.L. Chen, Z. Yang, J. Alloys Compd. 509 (2011) 1880–1884.
[4] S. Chen, X.H. Zhou, S.R. Zhang, B. Li, T. Zhang, J. Alloys Compd. 505 (2010) 613–618.
[5] M.R. Joung, J.S. Kim, M.E. Song, S. Nahm, J.H. Paik, J. Am. Ceram. Soc. 93 (2010) 934–936.
[6] C.L. Huang, C.L. Pan, W.C. Lee, J. Alloys Compd. 462 (2008) L5–L8.
[7] D. Zhou, C.A. Randall, L.X. Pang, H. Wang, X.G. Wu, J. Guo, G.Q. Zhang, L. Shui, X. Yao, J. Am. Ceram. Soc. 94 (2011) 802–805.
[8] C.L. Huang, J.Y. Chen, C.Y. Jiang, J. Am. Ceram. Soc. 93 (2010) 2755–2759.
[9] S. George, M.T. Sebastian, J. Alloys Compd. 473 (2009) 336–340.
[10] S.H. Kweon, M.R. Joung, J.S. Kim, B.Y. Kim, S. Nahm, J.H. Paik, Y.S. Kim, T.H. Sung, J. Am. Ceram. Soc. 94 (2011) 1995–1998.
[11] J.X. Tong, Q.L. Zhang, H. Yang, J.L. Zou, J. Am. Ceram. Soc. 90 (2007) 845–849.
[12] J.B. Lim, M.H. Kim, J.C. Kim, S. Nahm, J.H. Paik, J.H. Kim, Jpn. J. Appl. Phys. 45 (2006) L242–L244.
[13] C.L. Huang, Y.H. Chien, J. Alloys Compd. 509 (2011) L293–L295.
[14] Q.L. Zhang, H. Yang, H.P. Sun, J. Eur. Ceram. Soc. 28 (2008) 605–609.
[15] Q.L. Zhang, D. Zou, H. Yang, J. Eur. Ceram. Soc. 31 (2011) 265–272.
[16] J.S. Kim, N.H. Nguyen, J.B. Lim, D.S. Paik, S. Nahm, J.H. Paik, J.H. Kim, H.J. Lee, J. Am. Ceram. Soc. 91 (2008) 671–674.
[17] K.M. Manu, P.S. Anjana, M.T. Sebastian, Mater. Lett. 65 (2011) 565–567.
[18] D.J. Chu, L. Fang, H.F. Zhou, X.L. Chen, Z. Yang, J. Alloys Compd. 509 (2011) 1931–1935.
[19] X.L. Chen, H.F. Zhou, L. Fang, X.B. Liu, Y.L. Wang, J. Alloys Compd. 509 (2011) 5829–5832.
[20] J.R. Kim, D.W. Kim, H.S. Jung, K.S. Hong, J. Eur. Ceram. Soc. 26 (2006) 2105–2109.
[21] F. Gao, J.J. Liu, R.Z. Hong, Z. Li, C.S. Tian, Ceram. Int. 35 (2009) 2687–2692.
[22] M.H. Kim, Y.H. Jeong, S. Nahm, H.T. Kim, H.J. Lee, J. Eur. Ceram. Soc. 26 (2006) 2139–2142.
[23] H.F. Zhou, X.L. Chen, L. Fang, C.Z. Hu, H. Wang, J. Am. Ceram. Soc. 93 (2010) 1537–1539.
[24] H. Zhuang, Z.X. Yue, S.Q. Meng, F. Zhao, L.T. Li, J. Am. Ceram. Soc. 91 (2008) 3738–3741.
[25] S.J. Kim, E.S. Kim, Ceram. Int. 35 (2009) 137–141.
[26] N. Santha, M.T. Sebastian, Mater. Res. Bull. 43 (2008) 2278–2284.
[27] H. Zheng, I.M. Reaney, D. Muir, T. Price, D.M. Iddles, J. Eur. Ceram. Soc. 27 (2007) 4479–4487.
[28] J.B. Lim, K.H. Cho, S. Nahm, J.H. Paik, J.H. Kim, Mater. Res. Bull. 41 (2006) 1868–1874.
[29] Y. Zeng, H. Wang, H.F. Zhou, J. Mater. Res. 25 (2010) 2380–2383.
[30] S.B. Narang, S. Bahel, S. Dash, J. Mater. Sci. Mater. Electron. 21 (2010) 1186–1190.
[31] Q.H. Yang, E.S. Kim, P.K. Kim, Mater. Chem. Phys. 79 (2003) 236–238.
[32] C. Qin, Z. Yue, Z. Gui, L. Li, Mater. Sci. Eng. B 99 (2003) 286–289.
[33] K.H. Yoon, M.S. Park, J.Y. Cho, E.S. Kim, J. Eur. Ceram. Soc. 23 (2003) 2423–2427.
[34] G. Subodh, M.T. Sebastian, Mater. Sci. Eng. B 136 (2007) 50–56.
[35] R.L. Moreira, P.S.M. Lobo, G. Subodh, M.T. Sebastian, F.M. Matinaga, A. Dias, Chem. Mater. 19 (2007) 6548–6554.
[36] M. Yoshida, N. Hara, T. Takada, Jpn. J. Appl. Phys. 36 (1997) 6818–6823.
[37] H.L. Chen, C.L. Huang, Jpn. J. Appl. Phys. 41 (2002) 5650–5653.
[38] C.H. Wei, J.H. Jean, J. Am. Ceram. Soc. 86 (2003) 93–98.
[39] C.L. Huang, M.H. Weng, Mater. Res. Bull. 36 (2001) 2741–2750.
[40] C.L. Huang, K.H. Chiang, Mater. Sci. Eng. A 474 (2008) 243–246.
[41] B.S. Guiton, P.K. Davies, Nat. Mater. 6 (2007) 586–591.